symmetry

MDPI

Article

Fault Diagnosis for China Space Station Circulating Pumps: Prototypical Network with Uncertainty Theory

Wenbo Wu [1,2], Tianji Zou [1,2], Dong Guo [1,2], Lu Zhang [1,2,*], Ke Wang [1,2] and Xuzhi Li [1,2]

[1] Technology and Engineering Center for Space Utilization, Chinese Academy of Sciences, Beijing 100094, China; wuwenbo@csu.ac.cn (W.W.)
[2] The Key Laboratory of Space Utilization, 9 Dengzhuang South Road, Haidian Distirct, Beijing 100094, China
* Correspondence: zhanglu@csu.ac.cn

Abstract: Methods for fault diagnosis based on metric learning, in which a query sample is classified by picking the closest prototype from the support set based on their feature similarities, have been the subject of many studies. In real-world applications of in-orbit products, such as circulating pumps, the computation of similarity between different pairs is prone to different degrees of inaccuracy, especially epistemic uncertainty. Knowing and considering the uncertainty of similarity may improve fault detection accuracy. This article provides a unique approach to fault diagnosis based on Prototypical Network (Pro-Net) and Uncertainty Theory. In particular, we use epistemic uncertainty by altering the representation of prototypes from a deterministic scalar to an uncertain representation. To assess the similarity between a query and the prototypes in a support set, we calculate the uncertain distance between the pairs using cross-entropy. Experiments with symmetrical structures reveal that our proposed method significantly enhances classification precision and achieves state-of-the-art performance. It improves the reliability of fault diagnosis and reduces the risk of making erroneous judgments in safety-critical systems, decreasing the possibility of adverse consequences.

Keywords: circulating pumps; fault diagnosis; Prototypical Network; uncertainty theory; epistemic uncertainty; safety-critical

Citation: Wu, W.; Zou, T.; Guo, D.; Zhang, L.; Wang, K.; Li, X. Fault Diagnosis for China Space Station Circulating Pumps: Prototypical Network with Uncertainty Theory. *Symmetry* **2023**, *15*, 903. https://doi.org/10.3390/sym15040903

Academic Editors: Meilin Wen, Xiaoyang Li, Qingyuan Zhang and Tianpei Zu

Received: 13 March 2023
Revised: 4 April 2023
Accepted: 10 April 2023
Published: 13 April 2023

1. Introduction

China National Space Administration has finished building the T-shaped Tiangong orbiting outpost, comprising the Tianhe core module and the Wentian and Mengtian experiment modules [1]. With the experiment racks placed in the Experiment Modules, it is anticipated that the station, just the second laboratory in orbit, would host over a thousand scientific experiments for at least ten years. They include the study of microgravity's influence on novel materials, biological tissues, and basic physics. Since experiment modules must work within a certain range of temperatures, the thermal control subsystem is crucial in completing the abovementioned experiment. In addition, while discussing human spaceflight, various factors must be considered to secure people's lives throughout the voyage. Thus, the thermal control subsystem built for human flights is more crucial and sophisticated. Being crucial components of the thermal control subsystem, centrifugal pumps are susceptible to wear and have short lifespans. If the malfunction arises and is not recognized and remedied in time, it will have catastrophic repercussions for the space station and crew. Thus, fault diagnosis, timely detection, and treatment of circulating pumps must ensure the station's safe functioning over the next decade in orbit.

In the previous several decades, much research has been conducted on the fault diagnosis of circulating pumps. Various strategies have been created, spanning from model-based [2–4] to data-driven [5–9]. As the most popular method for fault diagnosis, Prototypical Networks (Pro-Net) have been utilized extensively. Prototypical Networks (Pro-Net) have the advantage of dealing with small samples without expanding the dataset with random noise or unlabeled samples, unlike traditional deep learning methods such as CNN [10] and RNN [11]. For bearing fault identification, He et al. [12] combined a kernel principal component analysis strategy with a semi-supervised prototype network (PSSPN), using unlabeled data to its maximum potential. Yu et al. [13] suggested a failure detection technique based on a mixed self-attention Prototypical Network that can acquire more discriminative characteristic information to learn the measurement prototypes of gearboxes in different health conditions. Zhang et al. [14] developed a feature distance-based deep prototype network (FDDPN) for few-shot defect detection in an open-set domain adaptation situation. Liu [15] suggested a fault diagnosis technique for gearboxes with noisy labels based on twin Prototypical Networks with label self-correction.

The fundamental procedure for Pro-Net is obtaining the prototype from raw measurement data using a probability metric. However, the probability metric [16] is limited in that it solely captures aleatory uncertainty (the intrinsic unpredictability of the actual world reflected by probability distributions [17]) and does not take epistemic uncertainty into account (uncertainty caused by our lack of knowledge [18,19]). In real-world scenarios, as a newly developed product with only a few samples, the circulation pump suffers from insufficient ground testing and large differences between ground testing and in-orbit operating environments, limiting knowledge on system fault diagnosis, and resulting in epistemic uncertainty. Thus, Pro-Net approaches that do not account for epistemic uncertainty cannot be used directly for practical applications, resulting in erroneous diagnostic findings. The uncertainty theory, developed by Liu [20] and detailing uncertain metrics for quantifying events with epistemic uncertainty, has been established. Regarding aleatory and epistemic uncertainty, Liu [21] widened the scope of the unsure measure to the chance measure.

We propose a novel defect diagnostic approach (Uncertainty Pro-Net) for centrifugal pumps based on Pro-Net and uncertainty theory as a result of the abovementioned study. The core concept of the Uncertainty Pro-Net method is to convert the representation of prototypes from a deterministic scalar to an uncertain representation by adding an epistemic uncertainty variable and then to classify faults using uncertainty metrics, such as uncertain distance, instead of probability metrics. By comparing the computational complexity and accuracy of the results of the suggested technique, we discover that the new method is more efficient and accurate in most circumstances.

The main highlights of the study are as follows:

(1) A new fault diagnosis method based on uncertainty theory is proposed, which captures an accurate understanding of aleatoric and epistemic uncertainties.
(2) Compared with other fault diagnosis methods, such as CNN (Convolutional Neural Network), the new method achieves more accurate and reliable diagnosis results when few labeled samples are available.
(3) The new method has been applied for the first time to the circulation pump of the space station. It can effectively diagnose four typical failure modes: bearing race wear, bearing roller wear, impeller wear, and bearing pre-stress slack.

The structure of the paper is as follows: Section 2 provides a concise introduction to uncertainty theory and Prototypical Network. Then, in Section 3, we describe the architecture of the proposed Uncertainty Pro-Net framework for fault diagnostics, along with model implementation details. Section 4 presents the test bed for centrifugal pumps and demonstrates the efficacy of our suggested technique. In this part, the suggested approach is also compared to other methods. Finally, conclusions are presented in Section 5.

2. Preliminaries

2.1. Uncertainty Theory

This part provides the relevant concepts and theorems to comprehend the suggested technique.

Uncertainty theory has been widely used as a fresh technique for describing epistemic (especially human) uncertainties. In uncertainty theory, belief degrees of events are quantified by establishing measures of uncertainty.

Theorem 1 ([22])**.** *Assume Γ is a nonempty set and $\mathcal{L}$ is an algebra over. If a set function $\mathcal{M}$ meets the following three axioms, it is an uncertain measure.*

Axiom2(Normality Axiom): $\mathcal{M}\{\Gamma\} = 1$ for the universal set Γ.
Axiom3(Duality Axiom): $\mathcal{M}\{\Lambda\} + \mathcal{M}\{\Lambda^c\} = 1$ for any event $\Lambda \in \mathcal{L}$.
Axiom4(Subadditivity Axiom): For every countable sequence of events, $\Lambda_1, \Lambda_2, \cdots$, we have

$$\mathcal{M}\left\{\bigcup_{i=1}^{\infty} \Lambda_i\right\} \leq \sum_{i=1}^{\infty} \mathcal{M}\{\Lambda_i\} \tag{1}$$

Theorem 2 ([23])**.** *A variable ξ is considered linear if its uncertainty distribution is linear.*

$$\Phi(x) = \begin{cases} 0, & if\ x \leq a \\ \frac{x-a}{b-a}, & if\ a \leq x \leq b \\ 1, & if\ x \geq b \end{cases} \tag{2}$$

Denoted by $\mathcal{L}[a, b]$, where a and b satisfy the inequality $a < b$.

Theorem 3 ([24])**.** *The inverse uncertainty distribution of the linear uncertain variables $\mathcal{L}[a, b]$ is*

$$\Phi^{-1}(\alpha) = (1 - \alpha)a + \alpha b \tag{3}$$

Theorem 4 ([25])**.** *Let ξ and η be independent uncertain variable with regular uncertainty distribution Φ and Ψ,respectively. Then the distance between ξ and η is*

$$d(\xi, \eta) = \int_0^1 \left|\Phi^{-1}(\alpha) - \Psi^{-1}(1 - \alpha)\right| d\alpha \tag{4}$$

2.2. Prototypical Network

Pro-Net [26] classifies an unknown instance into its closest class based on similarities with a few labeled samples, as is customary for similarity-based fault diagnostic algorithms. A neural network obtains an embedding function via prototype network learning; samples are extracted into feature vectors. The prototype is composed of the mean vectors of each class. Classification requires query samples to be transformed into feature vectors; the proximity of these vectors to the prototypes' vectors is a measure of how well they match that class. Figure 1 illustrates how the Pro-Net operates. The circle in the embedding space represents the embedded vector of each fault, and the classes are represented by red, orange, and blue, respectively. The star in the figure represents each principal characteristic.

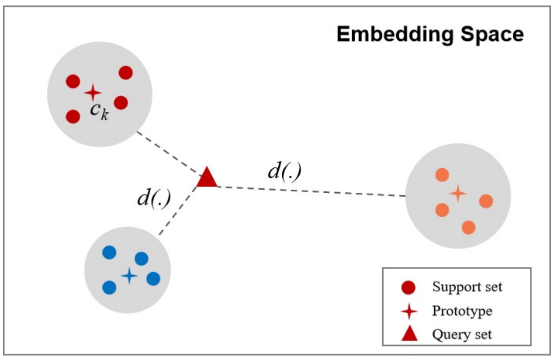

Figure 1. Schematic diagram of prototype network. (Different colors indicate different fault classes).

To acquire a feature vector as the embedding result of a feature extractor, we first input an image through the feature extractor to create a feature map. Then, prototypes are created for classes using the support set, where the feature embeddings of all class samples are averaged to get a value for class index k.

$$c_k = \frac{1}{|S_k|} \sum_{(x_i, y_i) \in S_k} f_\phi(x_i) \tag{5}$$

where x_i represents the query-sample indexed by i and y_i represents its label, S_k represents the collection of samples of the k-th class in the support set $S = \{S_1, \cdots, S_N\}$, and $f_\phi(\cdot)$ represents the quantity of samples in S_k.

We calculate the classification loss for a given query picture with ground-truth label as follows:

$$\mathcal{L}[x_i, y_i = k] = -\log\left(\frac{\exp(-d(f_\phi(x_i), c_k))}{\sum_k \exp(-d(f_\phi(x_i), c_k))}\right) \tag{6}$$

where $d(\cdot)$ represents the Euclidean distance between the given query-sample x_i and the prototype c_k of the class k.

3. Proposed Method

This work developed a defect diagnostic approach based on Pro-Net and uncertainty theory (Uncertainty Pro-Net). Figure 2 provides a full overview of the workflow of the suggested solution.

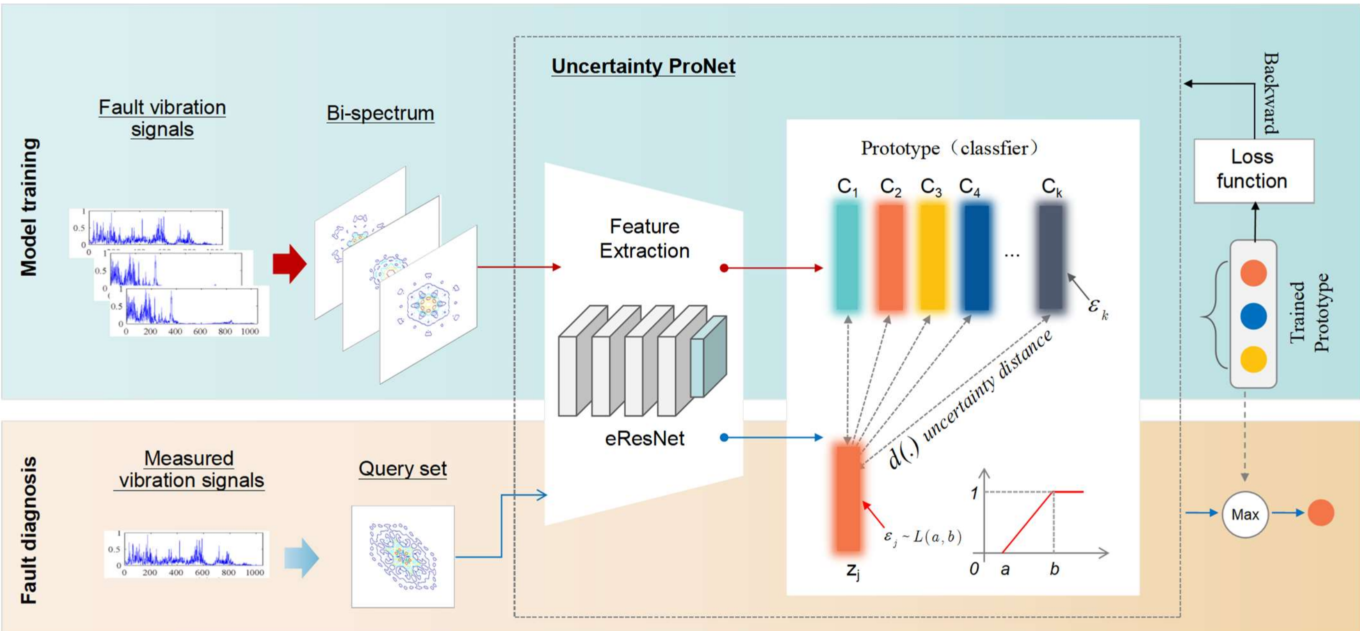

Figure 2. Fault diagnosis framework of the proposed method.

Part 1 converts the original vibration signals from 1D-dimensional signals to 2D pictures utilizing Bi-spectrums, which can suppress Gaussian-colored noise. First, separate these photos into a support and query set, then input them into Pro-Net to extract each class's primary characteristic (prototype).

Part 2 converts the deterministic scalar form of embedded query vectors and prototypes to an uncertain representation by adding an epistemic uncertainty variable. Next, compute the uncertainty distances between embedded query vectors and the prototypes of each class. Finally, compute the loss and adjust the network's settings. The pre-trained model is obtained by iteration.

Part 3, Through the pre-trained model, predict the label of test data. Fault classification can be achieved.

3.1. Bi-spectrum

Bi-spectrum is the Fourier transform of a cumulant of the third order [27]. The order of the bi-spectrum is the lowest in the high-order spectrum. Hence it is the most simple and practical. In this research, $\{x(n)\}$ it was defined as a non-stationary random signal with zero means, and its autocorrelation function was defined as follows:

$$r(\tau) = E\{x(n)x(n+\tau)\} \tag{7}$$

where $E\{x(n)x(n+\tau)$ is the mathematical expectation. The definition of a power spectrum is the Fourier transform of an autocorrelation function:

$$p(w) = \sum_{-\infty}^{+\infty} r(\tau)\exp\{-j(w\tau)\} \tag{8}$$

The momentum of the third order is defined as:

$$R(\tau_1, \tau_2) = \{x(n) \times (n+\tau_1) \times (n+\tau_2)\} \tag{9}$$

The 2D Fourier transform of the third moment is characterized by a bi-spectrum.

$$B(\omega_1, \omega_2) = \sum_{\tau_1=-\infty}^{+\infty} \sum_{\tau_2=-\infty}^{+\infty} R(\tau_1, \tau_2) \times e^{\{-j(w_1\tau_1 + w_2\tau_2)\}} \tag{10}$$

A bispectrum of $\{x(n)\}$ can be approximated as:

$$B(\omega_1, \omega_2) = X(\omega_1)X(\omega_2)X(\omega_1 + \omega_1) \tag{11}$$

where $X(\omega)$ is the Fourier transform of $x(n)$.

3.2. Uncertainty Pro-Net

The uncertainty of a query-prototype pair's similarity is characterized by shifting the representation of c_k and z_j from a deterministic scalar to an uncertainty representation. We enable a differentiable representation of c_k and z_j by re-parameterizing it as:

$$\begin{aligned} \xi_k &= c_k + \varepsilon_k \\ \eta_j &= z_j + \varepsilon_j \end{aligned} \tag{12}$$

ε_k and ε_j denotes the epistemic uncertainty of prototype and query, respectively. We define them following a linear uncertainty distribution.

Compared to previous studies that used cosine distance for distance metrics between query-prototype pairs. In this paper, we use cross-entropy as the distance metrics. For example, the cross-entropy of ξ from η can be written as:

$$d_{ij} = D[\xi, \eta] = \int_{-\infty}^{+\infty} (\phi_\xi(x)\ln(\frac{\phi_\xi(x)}{\phi_\eta(x)}) + (1-\phi_\xi(x))\ln(\frac{1-\phi_\xi(x)}{1-\phi_\eta(x)}))dx \tag{13}$$

Since ε_k and ε_j follows linear distribution, it is known by definition that ξ_k and η_j also follows the linear distribution. Suppose that ξ_k and η_j follows uncertainty distributions $L(a,b)$ and $L(c,d)$ ($b \geq a, d \geq c$), respectively. Then the cross-entropy ξ from η is [28]:

$$\begin{aligned} d_{ij} = D[\xi, \eta] = \textstyle\int_a^b (\frac{x-a}{b-a}\ln\frac{(x-a)(d-c)}{(b-a)(x-c)} + \frac{b-x}{b-a}\ln\frac{(b-x)(d-c)}{(b-a)(d-x)})dx \\ + \textstyle\int_c^a \ln\frac{d-c}{d-x}dx + \int_b^d \ln\frac{d-c}{x-c}dx \end{aligned} \tag{14}$$

For a query image x, the probability of classifying it into the class k is:

$$p(y_i = k|x_i) = \frac{\exp(\tau \cdot d(f_\phi(x_i), c_k))}{\sum_{j=1}^{N} \exp(\tau \cdot d(f_\phi(x_i), c_j))} \quad (15)$$

where N is the number of classes in the support set and τ is a hyper-parameter (i.e., N-way). The $d(f_\phi(x_i), c_k)$ indicates how closely the provided query-sample x_i resembles the class k prototype c_k. Here, a similarity-based classifier is built using the N prototypes from the support set's N classes.

Algorithm 1 describes the whole algorithm.

Algorithm 1: Uncertainty Pro-Net strategy

Input: support set S_k, query set Q_e
Output: Fault diagnosis result $p(y_i = k|x_i^T)$

1. Preprocess the original vibration signals with Bi-spectrum.
2. For each class, do:
3. Select N classes from the dataset randomly; each class includes K samples from the support set S_k.
4. Obtain samples x_i^S and x_i^Q from support set S_k and query set Q_e, respectively and generate the support feature set $f_\phi(x_i^S)$ and query feature set $f_\phi(x_i^Q)$
5. Generate prototype c_k through Equation (5)
6. Discretizing the query vectors and prototypes by adding epistemic uncertainty variables ε_k and ε_j
7. Using the uncertainty distance metric, calculate the classification probability $p(y_i = k\left|x_i^Q\right.)$
8. Calculate the loss, and update the learnable parameter of Pro-Net
9. Use the model pre-trained in steps 2–8 to predict the classification probability of the test dataset.
10. End

4. Case Study

4.1. Data Acquisition

Using fault diagnostic tests on circulating pumps, the efficiency of the suggested diagnosis approach based on the Pro-Net and uncertainty theory was shown in this work. Figure 3 depicts the fault test bench for circulating pumps, which consisted primarily of a circulating pump, its associated equipment, and a signal-collecting system from which the experimental data were collected. The centrifugal pump is powered by a brushless DC motor, is self-lubricating, and has a dynamic seal design to provide a long and steady operation in orbit. The particular parameters are detailed in Table 1. By substituting invalid components, the fault test bench may mimic various failure types for learning fault diagnosis procedures. Included among the failure types that may be simulated are bearing race wear, bearing roller wear, impeller wear, and bearing pre-stress slack.

Table 1. Particular parameters of circulating pumps.

No.	Parameter Settings	Value	No.	Parameter Settings	Value
1	Rated flow rate	600 L/h	1	Rated speed	7000 r/min
2	Inlet pressure	0.17 MPa	2	Leakage rate	$\leq 1 \times 10^{-7}$ Pa·m^3/s
3	Lifting capacity	220 kPa	3	Power consumption	≤159 Kw

During the test, the bearing working speed was 7000 r/min, and the vibration signal was captured at 10,600 Hz. Vibration data are recorded under normal and fault circumstances, including bearing roller wear, impeller wear, and bearing pre-stress slack fault conditions. Each set is sampled for 2 s, and one set is gathered every 5 s.

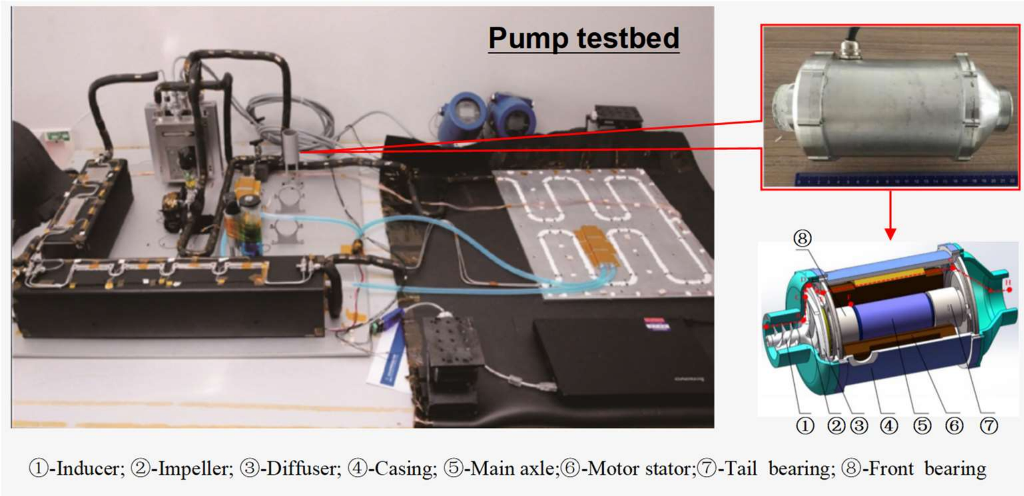

Figure 3. Single-phase fluid circuits circulating pump testbed.

4.2. Signal Processing by Bi-spectrum

The bi-spectrum counter maps of bearing roller wear, bearing ball wear, impeller wear fault state, and normal circumstances are shown in Figure 4a–d. The image illustrates considerable variances between the various fault modes, which may be utilized to distinguish between fault kinds.

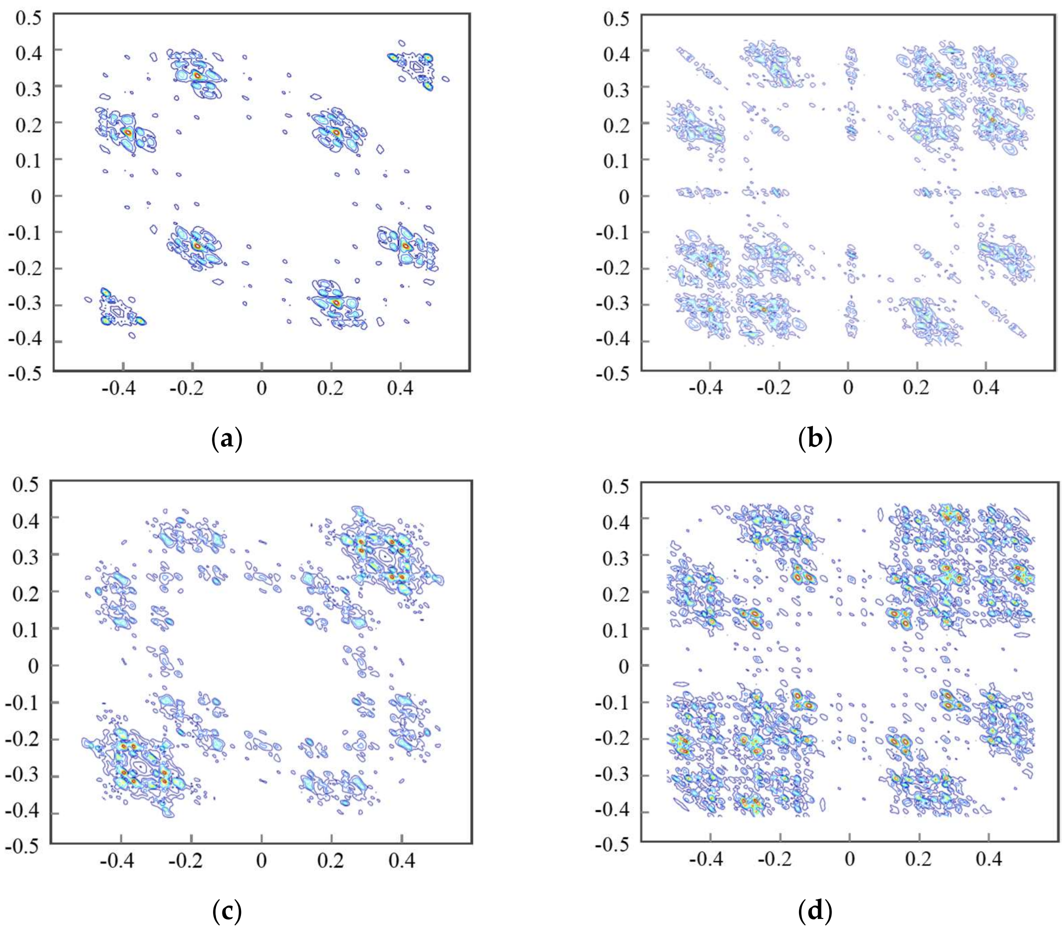

Figure 4. Bearing bi−spectrum chart: (**a**) Bearing race wear fault condition; (**b**) Bearing rollers wear fault condition; (**c**) Impeller wear fault condition; (**d**) Bearing pre−stress slack fault condition.

4.3. Networks and Training

The eResNet [29] network turns the bi-spectrum into a 128−dimensional vector throughout the experiment. Each residual block consists of three 3×3 convolutional layers and a 2×2 maximum pooling layer. The network consists of four residual blocks and a 1×1 convolutional layer with an average pooling layer. Figure 5 depicts the whole network architecture. The architectures of embedding networks of eResNet are shown in Table 2.

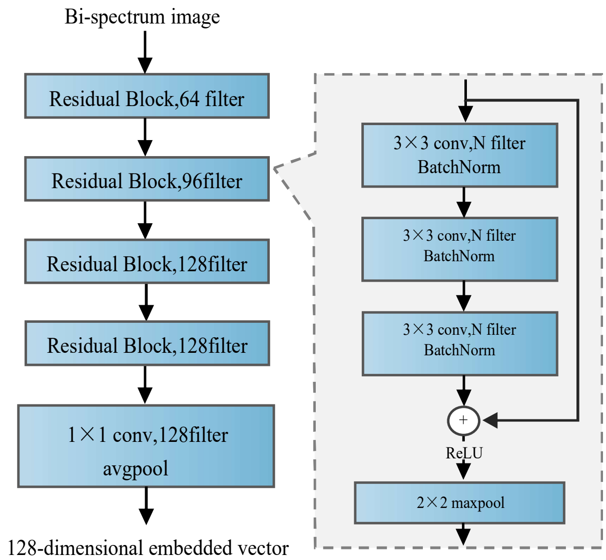

Figure 5. eResNet embedding network using the residual block.

Table 2. The architecture of embedding networks of eResNet.

Model Name	eResNet
Architecture	$\begin{bmatrix} C:3\times 3,64 \\ C:3\times 3,64 \\ C:3\times 3,64 \\ MP:2\times 2 \end{bmatrix} \begin{bmatrix} C:3\times 3,96 \\ C:3\times 3,96 \\ C:3\times 3,96 \\ MP:2\times 2 \end{bmatrix} \begin{bmatrix} C:3\times 3,128 \\ C:3\times 3,128 \\ C:3\times 3,128 \\ MP:2\times 2 \end{bmatrix} \times 2$
Parameter layers	13
Parameters	1.24×10^6

In image learning, 50, 100, and 200 training examples were chosen to feed the uncertainty Pro-Net. At each iteration, the support set is picked randomly from the samples, the number of support sets is set to 10, and the remaining samples are utilized as the query set. We used a Squama Model in [30] to quantify the epistemic uncertainty factor (EUF). The results are shown in Table 3.

Table 3. Epistemic uncertainty factor assumed in this paper.

Failure Mode	EUF	Failure Mode	EUF
Bearing race wear	$\varepsilon_e \sim L(2,5)$	Impeller wear	$\varepsilon_e \sim L(3,7)$
Bearing rollers wear	$\varepsilon_e \sim L(5,8)$	Bearing pre-stress slack	$\varepsilon_e \sim L(9,11)$

4.4. Fault Diagnosis and Results

When the model has been completely trained according to the approach shown in Figure 1, the validation set verifies the model's performance in defect identification using real centrifuge data. The validation set has ten samples, and the number of iterations is also set at 10. The final diagnostic result was determined by averaging the ten instances of correctness to limit the impact of random elements.

The Uncertainty Pro-Net approach has high accuracy in diagnosing four different fault modes. The experimental data to verify that the samples whose probability value was greater than 0.7 had high classification accuracy, as shown in Figure 6.

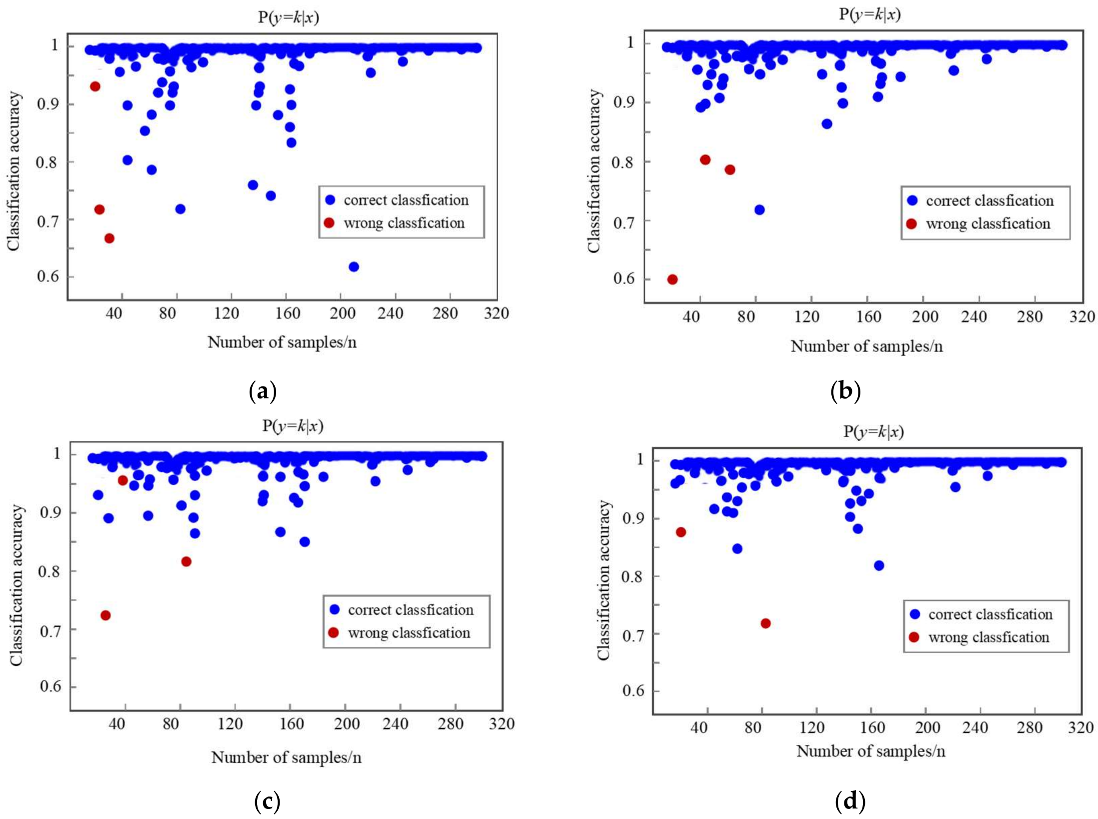

Figure 6. Fault diagnosis accuracy under different fault modes: (**a**) Bearing race wear fault condition; (**b**) Bearing rollers wear fault condition; (**c**) Impeller wear fault condition; (**d**) Bearing pre-stress slack fault condition.

The value of the loss function recorded to characterize the performance of the model is calculated to estimate the convergence of the algorithm, shown in Figure 7. In the beginning, losses decrease dramatically, which means the model has not found the direction for the optimal solution. Then the loss ascends gradually with the increase of iteration. Finally, from about the 120th iteration, losses reduce slowly and converge to 0 around, which indicates the model has been well-trained.

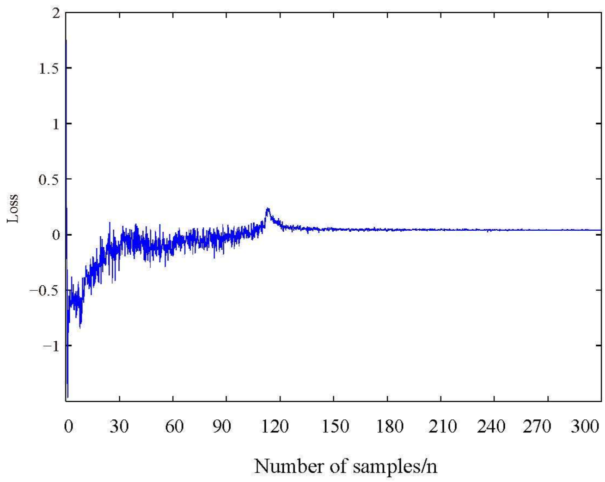

Figure 7. The loss curve of the Uncertainty Pro-Net model.

4.5. Comparison of Experimental Results

(1) Convolutional Neural Network (CNN) [31]: A traditional machine learning model that can directly classify data without preprocessing. A large number of samples are needed as a training set.
(2) Bispectral Neural Networks (BNN) [32]: The BNN method is proposed based on the CNN method and can simultaneously learn a group-equivariant Fourier transform and its corresponding group-invariant bispectrum.
(3) Prototypical Network (Pro-Net) [33]: The Pro-Net method is a typical metric-based few-shot learning method, which classifies an unseen instance into its nearest class based on the similarities with a few labeled examples.
(4) Uncertainty Pro-Net: The new approach proposed by this article can take both aleatoric and epistemic uncertainties into consideration in the process of fault diagnosis.

Figure 8 illustrates the block diagram for our experiment.

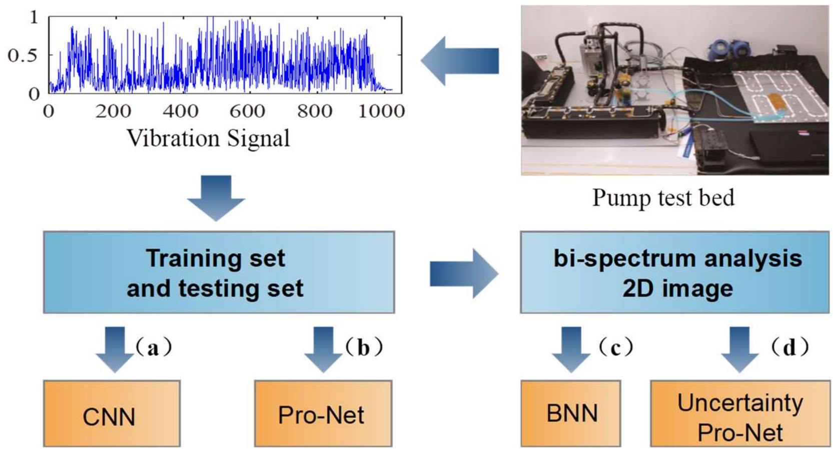

Figure 8. Flow chart of the experiment: (**a**) Convolutional Neural Network (CNN); (**b**) Prototypical Network (Pro-Net); (**c**) Bispectral Neural Networks (BNN); (**d**) Uncertainty Pro-Net.

We conducted trials comparing the aforementioned models using the same data set and equipment with sample sizes of 10, 50, 100, and 200. To guarantee the correctness of the experimental findings, we repeated the experiment under each sample 10 times and calculated the final accuracy rate by averaging the ten results. Table 4 shows the average accuracy of each model.

Table 4. Average diagnostic accuracy.

Methods	10	50	100	150	300
CNN	38.71 ± 0.16%	42.41 ± 0.41%	54.08 ± 0.01%	83.36 ± 0.14%	92.15 ± 0.24%
BNN	40.25 ± 0.53%	44.24 ± 0.18%	49.05 ± 0.06%	64.02 ± 0.14%	70.82 ± 0.29%
Pro-Net	63.59 ± 2.20%	67.89 ± 1.91%	80.74 ± 0.07%	84.84 ± 0.04%	90.42 ± 0.20%
Uncertainty Pro-Net	70.24 ± 0.30%	83.04 ± 0.06%	88.18 ± 0.08%	90.25 ± 0.04%	91.17 ± 0.03%

Figure 9 indicates that as the number of training samples rises, the accuracy of the four models will improve. Unfortunately, the accuracy of typical machine learning algorithms, whether CNN or BNN, is poor. This is because standard machine learning approaches can only obtain effective results with adequate training data. When the number of training samples increases, the accuracy rate of BNN decreases. BNN's topology is overly complicated, leading to severe overfitting. Pro-Net has always maintained a high degree of accuracy and uncertainty as a meta-learning technique, even with a sample size of 10. In addition, since Bispectral analysis decreases background noise greatly and accounts for epistemic uncertainty, the accuracy rate of uncertainty Pro-Net rose even more. In these four instances, the classification accuracy of Uncertainty Pro-Net exceeded that of Pro-Net. The improvement is most noticeable in the sample size of 50, which is 15.15%. As the number of training samples increased, the difference between the two models steadily shrunk to 7.44%, 5.45%, and 0.75%. This demonstrates that Uncertainty Pro-Net outperforms typical machine learning models and meta-learning in scenarios with small sample sizes and high background noise.

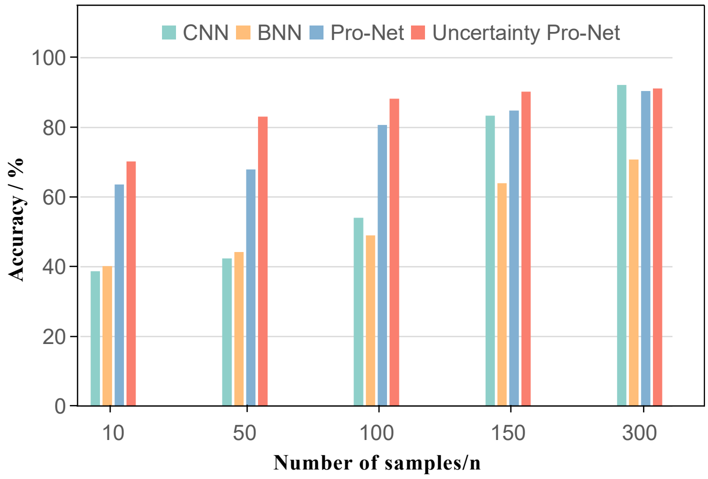

Figure 9. Diagnosis results with different sample sizes.

We created a confusion matrix to analyse the consistency and reliability of these four models in further depth. The confusion matrix is shown in Figure 10. Each model was repeated 3 times. Although containing some learning potential, CNN cannot maximise its advantages owing to a small sample size. BNN almost loses its capacity to classify. This is a result of the intricacy of the BNN structure and the vast number of trainable parameters. The results of BNN are almost random. In contrast, Pro-net and Uncertainty Pro-net are both stable. This illustrates that the model based on meta-learning can learn the capacity to learn, not just a specific classification task and that Uncertainty Pro-Net is more stable and less error-prone than Pro-Net.

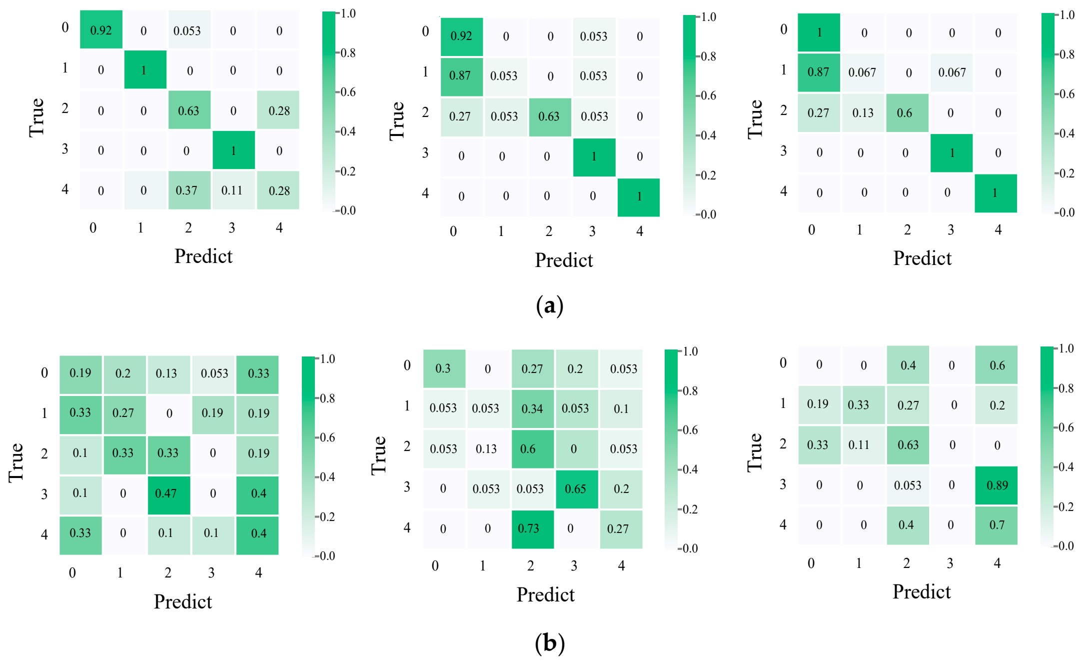

Figure 10. *Cont*.

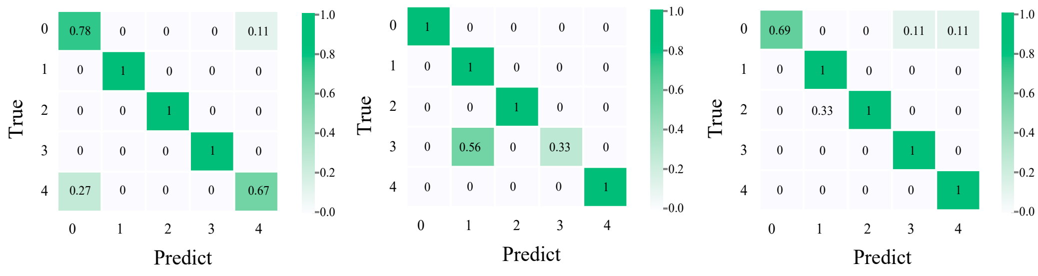

(**c**)

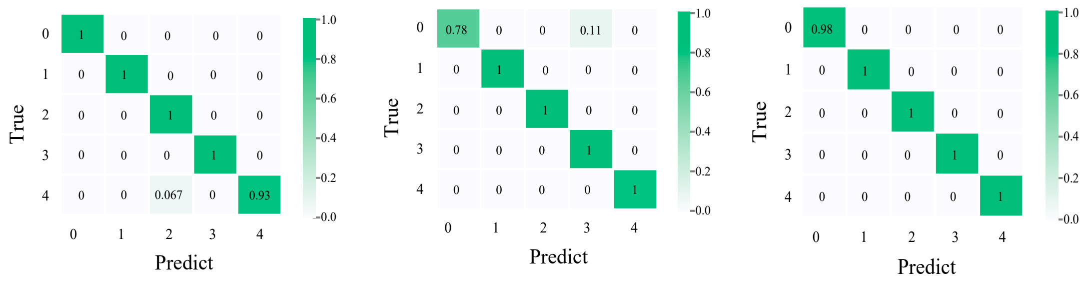

(**d**)

Figure 10. Confusion matrix of several models mentioned in the paper (each model repeated three times): (**a**) Convolutional Neural Network (CNN); (**b**) Bispectral Neural Networks (BNN); (**c**) Prototypical Network (Pro-Net); (**d**) Uncertainty Pro-Net.

5. Conclusions

Combining uncertainty theory with the Pro-Net approach yields a novel defect diagnostic technique.

(1) The dual-spectrum analysis method can convert the one-dimensional vibration signal with complex components into a clear and suitable two-dimensional image with good noise cancellation capability, highlighting the fault feature information more in the centrifuge's environment of strong background noise.

(2) The Uncertainty Pro-Net approach categorizes the health state of the query sample using uncertainty metric learning. Compared to conventional deep learning techniques such as CNN, the novel approach provides superior fault classification processing capabilities and more precise outputs. In particular, the new formula is symmetrical to the former formula, which shows that when it is too intricate to deal with a problem using the former formula, the problem can be observed from another perspective by using the new formula. New ideas may be obtained from the combination of uncertainty theory and symmetry.

(3) The Uncertainty Pro-Net approach has considerable relevance in engineering practice. Due to the vastly different ground test environment and in-orbit operational environment, circulating pumps have confusing fault perceptions. Without incorporating epistemic uncertainty in defect identification, such safety-critical products face severe repercussions.

Author Contributions: Conceptualization, X.L. and K.W.; methodology, W.W.; software, T.Z.; validation, W.W.; formal analysis, D.G.; investigation, D.G.; resources, K.W.; data curation, W.W.; writing—original draft preparation, W.W.; writing—review and editing, X.L.; visualization, W.W.; supervision, X.L.; project administration, L.Z.; funding acquisition, K.W. All authors have read and agreed to the published version of the manuscript.

Funding: This research received no external funding.

Data Availability Statement: Data available on request from the authors.

Conflicts of Interest: The authors declare no conflict of interest.

References

1. Gu, Y. The China Space Station: A new opportunity for space science. *Natl. Sci. Rev.* **2022**, *9*, nwab219. [CrossRef] [PubMed]
2. Ekanayake, T.; Dewasurendra, D.; Abeyratne, S.; Ma, L.; Yarlagadda, P. Model-based fault diagnosis and prognosis of dynamic systems: A review. *Procedia Manuf.* **2019**, *30*, 435–442. [CrossRef]
3. Mouzakitis, A. Classification of Fault Diagnosis Methods for Control Systems. *Meas. Control.* **2013**, *46*, 303–308. [CrossRef]
4. Jamadar, I.M.; Bellary SA, I.; Kanai, R.A.; Alrobaian, A.A. Model-based condition monitoring for the detection of failure of a ball bearing in a centrifugal pump. *J. Fail. Anal. Prev.* **2019**, *19*, 1556–1568. [CrossRef]
5. Mushtaq, S.; Islam, M.M.; Sohaib, M. Deep learning aided data-driven fault diagnosis of rotatory machine: A comprehensive review. *Energies* **2021**, *14*, 5150. [CrossRef]
6. Li, T.; Zhao, Y.; Zhang, C.; Luo, J.; Zhang, X. A knowledge-guided and data-driven method for building HVAC systems fault diagnosis. *Build. Environ.* **2021**, *198*, 107850. [CrossRef]
7. Lada, E.K.; Lu, J.C.; Wilson, J.R. A wavelet-based procedure for process fault detection. *IEEE Trans. Semicond. Manuf.* **2002**, *15*, 79–90. [CrossRef]
8. Forouzanfar, M.; Safaeipour, H.; Casavola, A. Oscillatory Failure Case detection in flight control systems via wavelets decomposition. *ISA Trans.* **2022**, *128*, 47–53. [CrossRef]
9. Forouzanfar, M.; Khosrowjerdi, M.J. A Constrained Optimization Approach to Integrated Active Fault Detection and Control. *Iran. J. Sci. Technol. Trans. Electr. Eng.* **2017**, *41*, 229–240. [CrossRef]
10. Kumar, A.; Gandhi, C.P.; Zhou, Y.; Kumar, R.; Xiang, J. Improved deep convolution neural network (CNN) for the identification of defects in the centrifugal pump using acoustic images. *Appl. Acoust.* **2020**, *167*, 107399. [CrossRef]
11. Wu, W.; Zhang, L.; Fu, H.; Wang, K.; Li, X. Safety impact analysis considering physical failures and cyber-attacks for mechanically pumped loop systems (MPLs). *Sensors* **2022**, *22*, 4780. [CrossRef] [PubMed]
12. Zhao, Q.; Cheng, G.; Han, X.; Liang, D.; Wang, X. Fault Diagnosis of Main Pump in Converter Station Based on Deep Neural Network. *Symmetry* **2021**, *13*, 1284. [CrossRef]
13. He, J.; Zhu, Z.; Fan, X.; Chen, Y.; Liu, S.; Chen, D. Few-Shot Learning for Fault Diagnosis: Semi-Supervised Prototypical Network with Pseudo-Labels. *Symmetry* **2022**, *14*, 1489. [CrossRef]
14. Yu, H.; Tang, B.; Zhang, K.; Tan, Q.; Wei, J. Fault diagnosis method of wind turbine gearboxes mixed with attention Prototypical Network under small samples. *China Mech. Eng.* **2021**, *32*, 2475.
15. Zhang, X.; Wang, J.; Han, B.; Zhang, Z.; Yan, Z.; Jia, M.; Guo, L. Feature distance-based deep prototype network for few-shot fault diagnosis under open-set domain adaptation scenario. *Measurement* **2022**, *201*, 111522. [CrossRef]
16. Liu, X.; Tang, B.; Li, Q.; Yang, Q. Twin Prototypical Network with noisy label self-correction for fault diagnosis of wind turbine gearboxes. *Meas. Sci. Technol.* **2022**, *34*, 035006. [CrossRef]
17. Zhang, Z.; Lan, C.; Zeng, W.; Chen, Z.; Chang, S.F. Uncertainty-aware few-shot image classification. *arXiv* **2020**, arXiv:2010.04525.
18. Der Kiureghian, A.; Ditlevsen, O.; Der Kiureghian, A.; Ditlevsen, O. Aleatory or epistemic? Does it matter? *Struct. Saf.* **2009**, *31*, 105–112. [CrossRef]
19. Beer, M.; Ferson, S.; Kreinovich, V. Imprecise probabilities in engineering analyses. *Mech. Syst. Signal Process.* **2013**, *37*, 4–29. [CrossRef]
20. Aven, T.; Baraldi, P.; Flage, R.; Zio, E. *Uncertainty in Risk Assessment: The Representation and Treatment of Uncertainties by Probabilistic and Non-Probabilistic Methods*; John Wiley & Sons: Hoboken, NJ, USA, 2013.
21. Liu, B. *Uncertainty Theory: An Introduction to Its Axiomatic Foundation*; Physica-Verlag: Heidelberg, Germany, 2004.
22. Liu, Y. Uncertain random variables: A mixture of uncertainty and randomness. *Soft Comput.* **2013**, *17*, 625–634. [CrossRef]
23. Zhang, Q.; Kang, R.; Wen, M. Decomposition method for belief reliability analysis of complex uncertain random systems. *IEEE Access* **2019**, *7*, 132711–132719. [CrossRef]
24. Zhang, Q.; Zeng, Z.; Zio, E.; Rui, K. Probability box as a tool to model and control the effect of epistemic uncertainty in multiple dependent competing failure processes. *Appl. Soft Comput.* **2017**, *56*, 570–579. [CrossRef]
25. Kang, R.; Zhang, Q.; Zeng, Z.; Zio, E.; Li, X. Measuring reliability under epistemic uncertainty: Review on non-probabilistic reliability metrics. *Chin. J. Aeronaut.* **2016**, *29*, 571–579. [CrossRef]
26. Jia, L.; Yang, X.; Gao, X. A new definition of cross entropy for uncertain random variables and its application. *J. Intell. Fuzzy Syst.* **2018**, *35*, 1193–1204. [CrossRef]
27. Sun, C.; Paluri, M.; Collobert, R.; Nevatia, R.; Bourdev, L. Pro-Net: Learning to propose object-specific boxes for cascaded neural networks. In Proceedings of the IEEE Conference on Computer Vision and Pattern Recognition, Las Vegas, NV, USA, 27–30 June 2016; pp. 3485–3493.
28. Li, H. VMD Based Bi-spectrum for Bearing Fault Diagnosis. In *Advances in Natural Computation, Fuzzy Systems and Knowledge Discovery*; Springer International Publishing: Cham, Switzerland, 2021; pp. 357–364.
29. Chen, X.; Kar, S.; Ralescu, D.A. Cross-entropy measure of uncertain variables. *Inf. Sci.* **2012**, *201*, 53–60. [CrossRef]
30. Zheng, Y.; Wang, R.; Yang, J.; Xue, L.; Hu, M. Principal characteristic networks for few-shot learning. *J. Vis. Commun. Image Represent.* **2019**, *59*, 563–573. [CrossRef]
31. Tang, S.; Zhu, Y.; Yuan, S. A novel adaptive convolutional neural network for fault diagnosis of hydraulic piston pump with acoustic images. *Adv. Eng. Inform.* **2022**, *52*, 101554. [CrossRef]

32. Sanborn, S.; Shewmake, C.; Olshausen, B.; Hillar, C. Bispectral Neural Networks. *arXiv* **2022**, arXiv:2209.03416.
33. Jiang, C.; Chen, H.; Xu, Q.; Wang, X. Few-shot fault diagnosis of rotating machinery with two-branch prototypical networks. *Intell. Manuf.* **2023**, *34*, 1667–1681. [CrossRef]